Trine – A new limit on time reversal invariance violation in neutron beta decay

T. Soldner[1], L. Beck[2], C. Plonka[3], K. Schreckenbach[3], and O. Zimmer[4]

[1] Institut Laue Langevin, BP 156, F-38042 Grenoble Cedex 9, France
[2] Beschleunigerlabor von LMU und TU München, Am Coulombwall, D-85747 Arching, Germany
[3] Physik-Department E21, TU München, James-Franck-Str., D-85747 Arching, Germany
[4] Physik-Department E18, TU München, James-Franck-Str., D-85747 Arching, Germany

Summary. In neutron beta decay, the triple correlation between the neutron spin and the momenta of electron and antineutrino (D coefficient) tests for a violation of time reversal invariance beyond the Standard model mechanism of CP violation. We present a new preliminary limit for this correlation which was obtained by the Trine experiment: $D_{\mathrm{prel.}} = (-3.1 \pm 6.2^{\mathrm{stat}} \pm 4.7^{\mathrm{syst}} \pm 4.7^{\mathrm{syststat}}) \cdot 10^{-4}$.

1 Introduction

To create the baryon antibaryon asymmetry in the universe from a symmetric start, a baryon number, C and CP violating process outside thermal equilibrium is required [1]. CP violation was discovered in the decay of neutral kaons [2]. This type of CP violation is implemented in the Standard model of particle physics via a free phase in the quark mixing matrix [3] but seems to be insufficient to explain the observed baryon asymmetry [4].

Extensions of the Standard model like SUperSYmmetric models or Grand Unified Theories open new channels for CP violation which may be observed in low energy particle physics like in electric dipole moments (EDMs) or in the neutron beta decay. Especially the neutron EDM is a sensitive test for physics beyond the Standard model and restricts the parameter space for many alternative models [5]. The decay, however, namely the triple correlation D of the spin of the decaying neutron and the momenta of electron and antineutrino, is more sensitive for CP violation via leptoquarks [4] which appear naturally in GUTs.

The differential decay probability of the neutron can be written as [6]:

$$\frac{\mathrm{d}W}{\mathrm{d}E_{\mathrm{e}}\mathrm{d}\Omega_{\mathrm{e}}\mathrm{d}\Omega_{\bar{\nu}}} = gG_{\mathrm{E}}(E_{\mathrm{e}}) \left\{ 1 + a\frac{\boldsymbol{p}_{\mathrm{e}}\boldsymbol{p}_{\bar{\nu}}}{E_{\mathrm{e}}E_{\bar{\nu}}} + b\frac{m_{\mathrm{e}}}{E_{\mathrm{e}}} + \frac{\boldsymbol{\sigma}_{\mathrm{n}}}{\sigma_{\mathrm{n}}} \left(A\frac{\boldsymbol{p}_{\mathrm{e}}}{E_{\mathrm{e}}} + B\frac{\boldsymbol{p}_{\bar{\nu}}}{E_{\bar{\nu}}} + D\frac{\boldsymbol{p}_{\mathrm{e}} \times \boldsymbol{p}_{\bar{\nu}}}{E_{\mathrm{e}}E_{\bar{\nu}}} \right) \right\} \tag{1}$$

Here, g is a normalization constant, G_{E} the electron spectrum, $\boldsymbol{\sigma}_{\mathrm{n}}$ the neutron spin, E_i the energy, $\boldsymbol{p}_i$ the momentum, and $\mathrm{d}\Omega_i$ the solid angle of electron e and antineutrino $\bar{\nu}$, respectively. The coefficients a, b, A, B, and D describe the correlations between the decay products.

Eq. (1) assumes only Lorentz invariance but no discrete symmetries like parity P, charge conjugation C, or time reversal T. Indeed, the coefficients A and B are P and C violating and nonzero ($A = -0.1162(13)$, $B = 0.983(4)$ [7]). In the V–A-theory A or a are used to determine the ratio $|\lambda| := |g_{\mathrm{A}}/g_{\mathrm{V}}|$ of the axial vector and the vector coupling constant ($b \equiv 0$ in V–A-theory). Together with the neutron life time the absolute values of the coupling constants can be determined. For a precise measurement of the phase of λ, however, the D coefficient is required. A phase $\neq 0, \pi$, i.e. $D \neq 0$, would indicate T violation (and according to the CPT theorem CP violation). Up to now, no evidence for a deviation of D from 0 was found (world average $D = -0.6(1.0)\cdot 10^{-3}$ [7]). The Standard model prediction is $D < 10^{-12}$. Any value above the final state effect level ($D_{\mathrm{FS}} \approx 10^{-5}$ for neutrons) would indicate new physics. For leptoquark models, this experimental range is not excluded by measurements of alternative parameters (like, e.g., EDMs) [4].

2 Principle of a D measurement

To measure D in neutron decay, electron and proton (which can replace the antineutrino for slow neutrons) have to be detected dependent on the neutron spin. Integrating (1) over the acceptance of electron detector i and proton detector j gives the count rate $\dot{N}^{ij}$ of the detector combination $\mathrm{e}^i\mathrm{p}^j$:

$$\dot{N}^{ij} = \epsilon_{\mathrm{e}}^i \epsilon_{\mathrm{p}}^j \left\{ K_1^{ij} + aK_a^{ij} + bK_b^{ij} + \boldsymbol{P}\left(A\boldsymbol{K}_A^{ij} + B\boldsymbol{K}_B^{ij} + D\boldsymbol{K}_D^{ij} \right) \right\}. \tag{2}$$

Here, ϵ_{e}^i (ϵ_{p}^j) describes the detector efficiency of electron (proton) detector i (j). K_η^{ij} are apparatus constants that describe the sensitivity of the apparatus versus the coefficient $\eta \in \{1, a, b, A, B, D\}$, e.g.

$$K_1^{ij} \propto \left\langle \int_{\mathrm{e}^i\mathrm{p}^j} G_{\mathrm{E}}(E_{\mathrm{e}}) \mathrm{d}E_{\mathrm{e}} \mathrm{d}\Omega_{\mathrm{e}} \mathrm{d}\Omega_{\bar{\nu}} \right\rangle_V \quad \text{or} \quad \boldsymbol{K}_D^{ij} \propto \left\langle \int_{\mathrm{e}^i\mathrm{p}^j} G_{\mathrm{E}}(E_{\mathrm{e}}) \frac{\boldsymbol{p}_{\mathrm{e}} \times \boldsymbol{p}_{\bar{\nu}}}{E_{\mathrm{e}} E_{\bar{\nu}}} \mathrm{d}E_{\mathrm{e}} \mathrm{d}\Omega_{\mathrm{e}} \mathrm{d}\Omega_{\bar{\nu}} \right\rangle_V .$$

$\langle \ldots \rangle_V$ represents the average over the decay volume. $\boldsymbol{P}$ is the neutron polarization. Modifications are necessary for inhomogeneous ϵ or $\boldsymbol{P}$. The K_η can be determined by Monte Carlo simulations. The quotient

$$\alpha^{ij} := \frac{\dot{N}_\uparrow^{ij} - \dot{N}_\downarrow^{ij}}{\dot{N}_\uparrow^{ij} + \dot{N}_\downarrow^{ij}} = \boldsymbol{P}\left(A\boldsymbol{\kappa}_A^{ij} + B\boldsymbol{\kappa}_B^{ij} + D\boldsymbol{\kappa}_D^{ij} \right) \tag{3}$$

with $\boldsymbol{\kappa}_\eta^{ij} = \boldsymbol{K}_\eta^{ij}/(K_1^{ij} + aK_a^{ij} + bK_b^{ij})$ is independent on detector efficiencies.

Since $D \ll A, B$ the influence of the parity violating coefficients A and B has to be suppressed carefully. Therefore, the detector and the decay volume should have two common perpendicular mirror planes (x-z and y-z planes in Fig. 1 (a) which shows the simplest implementation). For such detector, A and B are suppressed to first order:

$$4P_z \kappa_{D,z} D = \alpha^{00} - \alpha^{01} - \alpha^{10} + \alpha^{11} =: \alpha_D. \tag{4}$$

This bases on the different symmetry properties of $\boldsymbol{\kappa}_A \propto \boldsymbol{p}_{\mathrm{e}}$, $\boldsymbol{\kappa}_B \propto \boldsymbol{p}_{\bar{\nu}}$, and $\boldsymbol{\kappa}_D \propto \boldsymbol{p}_{\mathrm{e}} \times \boldsymbol{p}_{\bar{\nu}}$. The detector is insensitive to a beam divergence and to deviations of the polarization from z axis. However, deviations from the mirror symmetries are sources for systematic errors. Whereas (4) suppresses the influences of the parity violating coefficients one can define asymmetries that enhance this influence and allow to investigate imperfections of the set-up:

$$\alpha_x := \alpha^{00} + \alpha^{01} - \alpha^{10} - \alpha^{11} = 4P_x(A\kappa_{A,x} + B\kappa_{B,x}) + 4P_y D\kappa_{D,y} \tag{5}$$
$$\alpha_y := \alpha^{00} - \alpha^{01} - \alpha^{10} + \alpha^{11} = 4P_y(A\kappa_{A,y} + B\kappa_{B,y}) + 4P_x D\kappa_{D,x} \tag{6}$$
$$\alpha_z := \alpha^{00} + \alpha^{01} + \alpha^{10} + \alpha^{11} = 4P_z(A\kappa_{A,z} + B\kappa_{B,z}). \tag{7}$$

The index of these combined asymmetries indicates the component of the polarization the asymmetry is sensitive to (cf. Fig. 1 (a)). In principle, (5)-(7) allow to derive the full polarization vector from the measured combined asymmetries, using the values for A and B from literature.

(a) 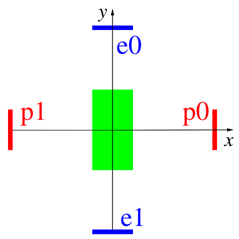

(b) 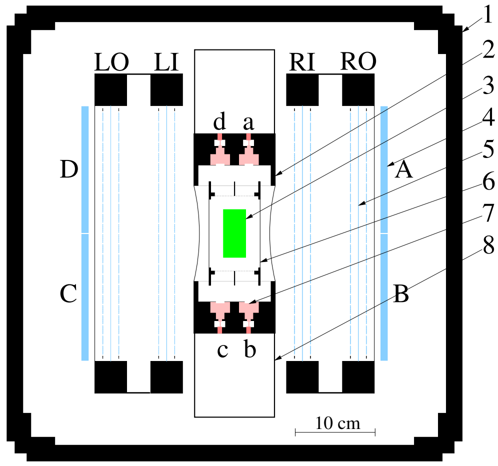

Fig. 1. (a) Simplest symmetric detector for D, (b) Cross section of the Trine detector: 1 – outer chamber (counting gas), 2 – inner vacuum chamber, 3 – neutron beam, 4 – plastic scintillator, 5 – wire chamber, 6 – electrode for proton acceleration, 7 – PIN diode, 8 – housing for PIN preamplifier. For both detectors, the polarizations points in z direction perpendicular to the plane of the drawing.

A further reduction of the sensitivity to the coefficients A and B can be obtained by optimizing the angle φ between electron and proton detector. This sensitivity can be described by $\kappa_A(\varphi)/\kappa_D(\varphi)$ and $\kappa_B(\varphi)/\kappa_D(\varphi)$ and has a minimum at slightly obtuse angles of about 120°, depending on the specific detector dimensions [8].

The statistical sensitivity of a combination of electron and proton detector is determined by the angular correlation between electron and proton and the dependence $\kappa_D = \kappa_D(\varphi)$ and has its maximum at about 135° [9, 8].

3 The Trine Experiment

Trine detects the electrons by 4 plastic scintillators ($560 \times 158 \times 8.5$ mm^3) in coincidence with multi wire proportional chambers and the protons after acceleration in a focusing electrostatic field by special PIN diodes with thin entrance windows (diameter of active area 10 mm, 25 nm dead layer; see [10] for the performance). Fig. 1 (b) shows a cross-section of the detector. The detector consists of 16 such planes which use the same four scintillators and wire chambers (Fig. 2). Only the central detector planes 03–14 and plane 16 were equipped with PIN diodes. Data analysis used the 12 central planes to avoid edge effects at the ends of the high voltage electrode. Plane 16 served to investigate these effects.

In each plane, four groups of detector combinations exist defined by the enclosed angle between electron and proton detector: 50°, 82°, 98°, and 130°. Each group fulfills the symmetries requested in section 2 (Fig. 1).

The experiment was carried out at the ILL cold neutron beam facility PF1. The beam polarization of $P = 0.974(26)$ was created by a focusing polarizer. The neutron spin was flipped every 3 s by a resonance flipper. An octagonal long coil (length 180 cm, diagonal 96 cm, correction coils at the ends), surrounded by a mu metal tube to shield the earth magnetic field, created the longitudinal spin holding field of 140 μT in the detector region. The field deviation $B_\perp/B_z$ from the z axis was smaller than $5 \cdot 10^{-3}$.

The neutron beam profile was measured at the beginning, the center and the end of the decay volume ($z = -15, 0, 15$ cm respectively) using gold foils which were exposed

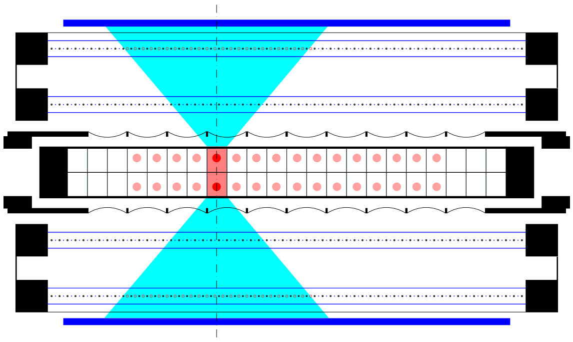

Fig. 2. Top view of the detector, symmetrization: The electron has to pass the wire chamber in a range symmetric to the PIN diode plane hit by the proton.

to the neutron beam and than scanned with an image plate [8]. The profile is slightly inhomogeneous in y direction (Fig. 3), caused by an inhomogeneous transmission of the focusing polarizer.

Data acquisition required the coincidence of a scintillator and the corresponding outer wire chamber. Thus, the trigger rate for events to store was kept low. Events without a wire chamber signal contributed a dead time of only 1.2 %. For each event, the analog signals of all scintillators, the numbers of the wires hit in all wire chambers, the number(s) and analog value(s) of the PIN diode(s) hit in the 10 μs after the second trigger, and the proton time of flight (TOF) between trigger and the first PIN diode hit were registered by a VME based acquisition system. The dead time per stored event was 30 μs, resulting in an overall dead time of 3.3 %. The VME bus was read out synchronously with the spin flip. Incomplete events (i.e. events without proton signal within the 10 μs) were sorted out by software. Only every 16th incomplete event was saved for control purposes. Monitor data like neutron flux, count rates of single detectors, high voltages of the electrode and the wire chambers were stored for each spin interval.

From the 100 days available at PF1 about 25 days in the first and 40 days in the second reactor cycle were used to collect statistics and 10 days of the second cycle for systematic tests. During the measurement, the scintillators were recalibrated every 10 days but only small adjustments were needed. Data from the first cycle suffered from high voltage problems and are not analysed yet. In the following we present the analysis of the data from the second cycle.

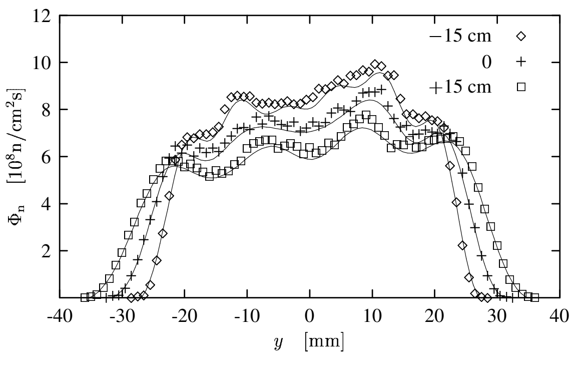

Fig. 3. Cuts of the beam profile (capture flux) in the decay volume in y direction. The solid lines correspond to 2 dimensional Fourier expansions of the data. The decay rate from this flux is about 10^3/s in the detector volume, resulting in a count rate of about 10/s (due to solid angle and electron-proton correlation).

4 Data Analysis

4.1 Selection of events

Spin intervals with unusual values of monitor signals together with the following three intervals and spin intervals where one VME module lost a trigger were removed (approx. 4 %). Only complete events with exactly one triggering PIN diode were used. A threshold of 150 keV was applied to the electron signal by software (hardware threshold was about 115 keV). The stability of the detectors was verified by an automatic generation of software cuts to the PIN analog spectra and allowed to sum the data to 10 days samples, corresponding to the period of scintillator recalibrations.

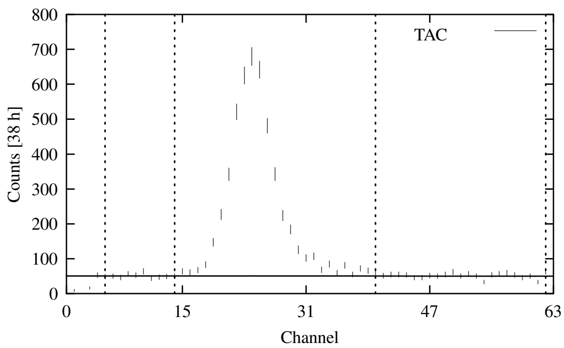

Fig. 4. Typical TOF spectrum (1 PIN diode and 1 scintillator for 98°). The dashed lines indicate the ranges for the background fit, the solid line the fit result.

Individual TOF spectra were calculated for all detector combination in each sample using the events that fulfill the software cuts. The background of the TOF spectra was fit by an exponential in a fixed range before and after the coincidence peak (Fig. 4). This shape of the background follows from the data acquisition which stopped the TOF measurement with the first proton signal. As a further consequence, the background behind the peak is suppressed compared to that in front of it. The χ^2 analysis showed perfect agreement between the exponential and the data for separate fits of the two fit ranges but a systematic increase to $\chi^2/\mathrm{ndf} = 1.26$ (averaged over all individual spectra) for a common fit of the ranges. To account for this the error of the background was scaled by a factor 1.124, but anyway the effect is very small due to the excellent signal to background ratio of 23 (averaged over the detector combinations used). The thus obtained peak areas were normalized with the neutron monitor counts of the particular spin to account for fluctuations caused by upstream experiments.

4.2 Selection of Detector Combinations

The measured count rates of the detector combinations 50° and 82° were higher than expected from the Monte Carlo simulations. These combinations are more sensitive to systematic effects due to the small particle energies caused by kinematics. This increases the scattering for electrons (e.g. by the counting gas). The low energy protons may be disturbed by a small penetration of the electrostatic field into the electrode. Furthermore, the sensitivity to A and B coefficient is larger for angles below 90° than for slightly obtuse angles, and the contribution of small angle combinations to the statistics can be neglected (see section 2 or [8]). Therefore, only the larger angle combinations (98° and 130°) were used in the analysis.

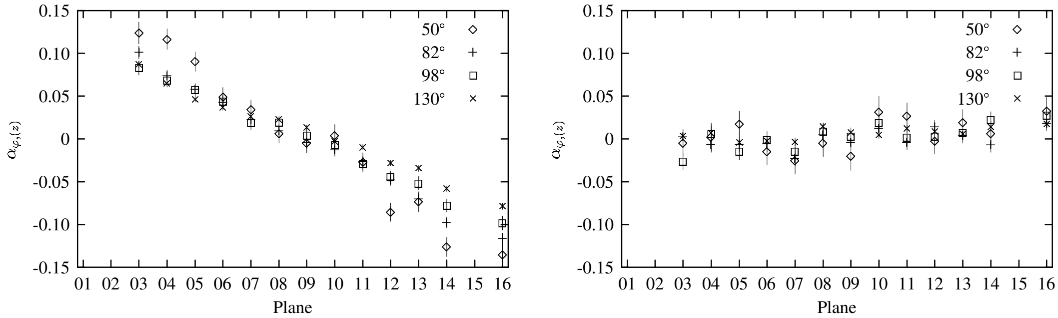

Fig. 5. Combined asymmetries $\alpha_z \approx 4\alpha$ as function of the detector plane. Left: full scintillator, right: symmetrized detector with ± 10 cm per plane.

4.3 Detector "Symmetrization"

The single asymmetry α^{ij} of a detector combination close to an end of the decay volume is high due to the spatial asymmetry of this combination in z direction, resulting in a sensitivity to A and B (Fig. 5, left). This sensitivity cancels by calculating the combined asymmetry α_D (section 2). However, for a real detector, effects like inhomogeneous detector efficiencies result in an incomplete cancellation which can fake $D \neq 0$. The spatial resolution of the wire chamber was used to suppress this sensitivity already in the initial asymmetries by selecting a symmetric electron detector range for each detector plane (see Fig. 2). The resulting asymmetries α_z are plotted in Fig. 5 (right). The size of the range was selected such that the variations of α_D between the different planes were consistent with statistical variations. For ± 10 cm a χ^2 of 10.4 (12.2) for 11 degrees of freedom was found for 98° (130°). The slightly higher χ^2 for 130° was taken into account as a systematic error of $2.2 \cdot 10^{-4}$. The change of the α_D values for different sizes of the wire chamber range was not fully compatible with statistics. Although this is expected since the range serves to suppress systematic effects it was considered as a contribution to the systematic error of $1.0 \cdot 10^{-4}$ by comparing the D values for different wire range sizes.

4.4 Influence of the Beam Profile

The influence of the beam profile was investigated with test measurements where one half or one quarter of the polarizer exit were closed to increase the beam shift (center of mass shifted by $\Delta y = 7.2$ mm for the 3/4 beam compared to 1 mm for the full beam). The results $D_{3/4}$ for the both detector combinations used were consistent with 0 but were used to limit the systematic error caused by the inhomogeneous beam profile: $\delta_{\text{shift}} D = 16(13) \cdot 10^{-4}$ $(2.4(5.0) \cdot 10^{-4})$ for 98° (130°) (statistical error given). A more precise calculation of this systematic error by Monte Carlo simulations is in progress and will replace the present estimation in the final result.

4.5 Results and Outlook

During the second cycle, $30 \cdot 10^6$ events were collected with the unshifted beam. $13.8 \cdot 10^6$ events fulfilled the symmetry condition (wire chamber range). The preliminary result is $D = (-3.1 \pm 6.2^{\text{stat}} \pm 4.7^{\text{syst}} \pm 4.7^{\text{syststat}}) \cdot 10^{-4}$. Syststat indicates the statistical error of the systematic error determined with the partially covered beam and will not enter into the final result after the Monte Carlo simulations (section 4.4). The systematic error consists

Table 1. Comparison of the latest D measurements.

	Year	P [%]	Events [10^6]	Sig/BG	D [10^{-3}]
[11]	1976	70(7)	6	4	-1.1 ± 1.7
[12]	1978	68(3), 65(1)	2.5	2.2	2.2 ± 3.0
emiT [9]	2000	96(2)	15	2.5	$-0.6 \pm 1.2 \pm 0.5$
Trine	2000	97.4(2.4)	30/13.8	23	$-0.31 \pm 0.62 \pm 0.47 \pm 0.47$

of the contributions given in sections 4.3 and 4.4 and those from the uncertainties of the apparatus constants ($0.3 \cdot 10^{-4}$) and polarization ($0.08 \cdot 10^{-4}$).

Table 1 compares the last D measurements. The result of the Trine measurement profits from the suppression of systematic effects using the spatial resolution of the wire chambers and the high segmentation with 12 used detector planes. Because of the signal to background ratio of 23 the statistics of the neutron beam could be used completely.

Improved measurements of emiT (Trine) are in progress (preparation). The world average for D may reach a precision in the very interesting lower 10^{-4} range within one year.

Acknowledgments

We are indebted to Prof. P. Liaud, Dr. A. Bussière, and Dr. R. Kossakowski for their help in the preparation of the experiment and for valuable discussions. We acknowledge the support of the Institut Laue Langevin. This work was supported by BMBF (grants 06 TM366 and 06TM879) and is associated to SFB 375 of the DFG.

References

1. A. D. Sakharov: JETP Lett. **5**, 24 (1967).
2. J. H. Christenson et al.: Phys. Rev. Lett. **13**, 138 (1964).
3. M. Kobayashi and T. Maskawa: Prog. Theo. Phys. **49**, 652 (1973).
4. P. Herczeg: Prog. Part. Nucl. Phys. **46** 413 (2001).
5. J. Ellis: NIM A **284** 33 (1989).
6. J. D. Jackson et al.: Phys. Rev. **106** 517 (1957).
7. K. Hagiwara et al.: Phys. Rev. D **66** 010001 (2002), `http://pdg.lbl.gov`.
8. T. Soldner: *Test der Zeitumkehrinvarianz am D-Koeffizienten des freien Neutronenzerfalls mit Trine*, phd-thesis, TU München (2001).
9. L. J. Lising et al.: Phys. Rev. C **62** 055501 (2000).
10. L. Beck et al.: in *Proc. of the ISINN 5 conference* 199, JINR, Dubna (1997).
11. R. I. Steinberg et al.: Phys. Rev. D **13** 2469 (1976).
12. B. G. Erozolimskii et al.: Sov. J. Nucl. Phys. **28** 48 (1978).